Plains CO_2 Reduction (PCOR) Partnership
Energy & Environmental Research Center (EERC)

IMPACTS OF LOCAL GRID REFINEMENT, CAPILLARY PRESSURE, AND RELATIVE PERMEABILITY ON EARLY INJECTION WELL BEHAVIOR DURING SIMULATION OF LARGE-DOMAIN DEDICATED CARBON DIOXIDE STORAGE

White Paper

Prepared for:

Joshua Hull

National Energy Technology Laboratory
U.S. Department of Energy (DOE)
626 Cochrans Mill Road
PO Box 10940, MS 921-107
Pittsburgh, PA 15236-0940

DOE Cooperative Agreement No. DE-FE0031838

Prepared by:

Thomas P. McGuire
Dominic C. Druke
Stephen N. Guillot
Merry D. Tesfu
Todd Jiang
Chantsalmaa Dalkhaa
Matthew L. Belobraydic
Nicholas W. Bosshart

Energy & Environmental Research Center
University of North Dakota
15 North 23rd Street, Stop 9018
Grand Forks, ND 58202-9018

November 2022

EERC DISCLAIMER

LEGAL NOTICE This research report was prepared by the Energy & Environmental Research Center (EERC), an agency of the University of North Dakota, as an account of work sponsored by the U.S. Department of Energy (DOE) National Energy Technology Laboratory (NETL) and the North Dakota Industrial Commission. Because of the research nature of the work performed, neither the EERC nor any of its employees makes any warranty, express or implied, or assumes any legal liability or responsibility for the accuracy, completeness, or usefulness of any information, apparatus, product, or process disclosed or represents that its use would not infringe privately owned rights. Reference herein to any specific commercial product, process, or service by trade name, trademark, manufacturer, or otherwise does not necessarily constitute or imply its endorsement or recommendation by the EERC.

ACKNOWLEDGMENT

This work was performed in support of the U.S. Department of Energy's SMART Initiative – Phase 1 through Leidos Inc.; IDIQ/Cost Reimbursable Term University (Federal) Subcontract Agreement; Subcontract No. P010227025; which supports Leidos' work under Prime Contract No. 89243318CFE000003; that has been issued by Department of Energy National Energy Technology Laboratory. This material is also based upon work supported by DOE Cooperative Agreement No. DE-FE0031838; "PCOR Initiative to Accelerate CCUS Deployment" and the North Dakota Industrial Commission (NDIC) under Contract Nos. FY20-XCI-226 and G-050-96. The authors also acknowledge the license of products from Computer Modelling Group, Calgary, Alberta, Canada.

DOE DISCLAIMER

This report was prepared as an account of work sponsored by an agency of the United States Government. Neither the United States Government, nor any agency thereof, nor any of their employees makes any warranty, express or implied, or assumes any legal liability or responsibility for the accuracy, completeness, or usefulness of any information, apparatus, product, or process disclosed or represents that its use would not infringe privately owned rights. Reference herein to any specific commercial product, process, or service by trade name, trademark, manufacturer, or otherwise does not necessarily constitute or imply its endorsement, recommendation, or favoring by the United States Government or any agency thereof. The views and opinions of authors expressed herein do not necessarily state or reflect those of the United States Government or any agency thereof.

NETL DISCLAIMER

This project was funded by the DOE National Energy Technology Laboratory, in part, through a site support contract. Neither the United States Government nor any agency thereof, nor any of their employees, nor the support contractor, nor any of their employees, makes any warranty, express or implied, or assumes any legal liability or responsibility for the accuracy, completeness, or usefulness of any information, apparatus, product, or process disclosed, or represents that its use would not infringe privately owned rights. Reference herein to any specific

commercial product, process, or service by trade name, trademark, manufacturer, or otherwise does not necessarily constitute or imply its endorsement, recommendation, or favoring by the United States Government or any agency thereof. The views and opinions of authors expressed herein do not necessarily state or reflect those of the United States Government or any agency thereof.

NDIC DISCLAIMER

This report was prepared by the EERC pursuant to an agreement partially funded by the Industrial Commission of North Dakota, and neither the EERC nor any of its subcontractors nor the North Dakota Industrial Commission nor any person acting on behalf of either:

(A) Makes any warranty or representation, express or implied, with respect to the accuracy, completeness, or usefulness of the information contained in this report or that the use of any information, apparatus, method, or process disclosed in this report may not infringe privately owned rights; or

(B) Assumes any liabilities with respect to the use of, or for damages resulting from the use of, any information, apparatus, method, or process disclosed in this report.

Reference herein to any specific commercial product, process, or service by trade name, trademark, manufacturer, or otherwise does not necessarily constitute or imply its endorsement, recommendation, or favoring by the North Dakota Industrial Commission. The views and opinions of authors expressed herein do not necessarily state or reflect those of the North Dakota Industrial Commission.

Plains CO_2 Reduction (PCOR) Partnership
Energy & Environmental Research Center (EERC)

IMPACTS OF LOCAL GRID REFINEMENT, CAPILLARY PRESSURE, AND RELATIVE PERMEABILITY ON EARLY INJECTION WELL BEHAVIOR DURING SIMULATION OF LARGE-DOMAIN DEDICATED CARBON DIOXIDE STORAGE

ABSTRACT

Results of large-domain carbon storage reservoir simulations conducted using a square grid initially showed early injection well pressure and rate trends inconsistent with typical carbon dioxide (CO_2), water, and gas injection well behavior measured in the field. To determine the potential cause of these differences, this simulation study was conducted to evaluate and quantify the relative effects of local grid refinement (LGR), relative permeability, and capillary pressure on long-term CO_2 injection well behavior. A large-domain (888-square mile) model of the Deadwood Formation (informally referred to as the Basal Cambrian) in the Williston Basin was used to simulate a single CO_2 injection well at two bottomhole injection pressures (BHIPs) with three different water–CO_2 relative permeability curves, both with and without capillary pressure. Without proper LGR, 12-year cumulative injected CO_2 mass is underpredicted by approximately 88% at a 90% fracture gradient BHIP. Reducing the BHIP requires smaller LGR cells to simulate expected early injection well behavior and indicates the need to review LGR for every realization of CO_2 injection, even after only changing BHIP or injection rate constraints. Error from excluding capillary pressure is observed to increase 12-year cumulative injection by 10% at a 90% fracture gradient BHIP and increases to 26% at the reduced BHIP. Finally, this study shows that relative permeability characterized by Bennion and Bachu,[1,2] provides similar simulation results compared to site-specific data at both explored BHIPs; therefore, these data can be temporarily used in place of site-specific data to accelerate the simulation-predicted CO_2 storage resource and injection rates.

[1] Bennion, B., and Bachu, S., 2007, Permeability and relative permeability measurements at reservoir conditions for CO_2–water systems in ultralow-permeability confining caprocks: Paper presented at the EUROPEC/EAGE Annual Conference and Exhibition, London, United Kingdom

[2] Bennion, B., and Bachu, S., 2005, Relative permeability characteristics for supercritical CO_2 displacing water in a variety of potential sequestration zones: Paper presented at the SPE Annual Technical Conference and Exhibition, Dallas, Texas.

TABLE OF CONTENTS

IMPACTS OF LOCAL GRID REFINEMENT (LGR), CAPILLARY PRESSURE, AND RELATIVE PERMEABILITY ON EARLY INJECTION WELL BEHAVIOR DURING SIMULATION OF LARGE-DOMAIN DEDICATED CARBON DIOXIDE STORAGE

EXECUTIVE SUMMARY

Reservoir simulators traditionally use finely gridded field sector models to predict reservoir response from oilfield operations. These simulations are typically dominated by microscopic fluid displacement (relative permeability) mechanisms, either during primary production or between injection and production wells during waterflooding or miscible/immiscible gas flooding, making relative permeability especially important.

In the past decade, these simulators have been adapted to predict reservoir and well behavior during carbon capture and storage (CCS) operations. CCS simulations require much larger simulation domain sizes to comply with CCS storage facility permit guidance to accurately predict the expected pressure elevation from large-scale carbon dioxide (CO_2) injection. Larger simulation domains have resulted in the use of simulation grid cells with X and Y dimensions that are about 10 times larger than typical oil production simulations to maximize efficiency and achieve large-domain simulation results within a reasonable computational time. However, the use of these large simulation grid cell sizes near wells causes simulated injection well pressure and rate behaviors to be inconsistent with those observed in typical subsurface fluid injection operations.

This white paper presents a simulation sensitivity study to demonstrate the relative effects of near-wellbore local grid refinement (LGR) at two different bottomhole injection pressure (BHIP) values: 90% of fracture gradient pressure (the maximum allowed for a carbon storage site [U.S. Environmental Protection Agency, 2018]) and significantly reduced BHIP. Presented data also show the relative effects of including capillary pressure and varying the relative permeability of the reservoir. Results from this study demonstrate not only the importance of LGR during carbon storage injection simulations but the need for an LGR region that extends beyond the parent cells penetrated by the injection well. Simulations with lower BHIP and correspondingly lower injection rates are observed to be significantly more sensitive to LGR X–Y cell dimensions and capillary pressures. Lower BHIP simulations also required smaller LGR cell dimensions but did not require a change In the LGR region size before typical injection well behavior was observed. Restraint should be exercised when expanding the LGR region around each well because the number of grid cells can increase exponentially as the LGR region is expanded, which can significantly impact computational time.

Without properly refined cells surrounding injection wells, simulations for this study showed 12-year cumulative injected CO_2 mass, an injection duration chosen to align with current 45Q CCS tax credits, is underpredicted by 88% at a 90% fracture gradient BHIP and more so at a reduced BHIP. To minimize error due to grid cell size in CCS reservoir simulations, this study recommends fit-for-purpose LGR cell dimensions and LGR regions around each well that extend beyond the parent cell of the injection well. Error from excluding capillary pressure is observed to increase 12-year cumulative injection of this study's simulations by 10% at a 90% fracture gradient BHIP and increases to 26% at reduced BHIPs. Therefore, capillary pressure should always be included

in final carbon storage simulations to avoid significantly overestimating injection capacity. Finally, this study shows that relative permeability characterized by Bennion and Bachu (2007, 2005) provides similar simulation results compared to site-specific data at both explored BHIPs, so these data can be temporarily used in place of site-specific data to accelerate the simulation-predicted CO_2 storage resource and injection rates.

Notes on White Paper

This white paper has been formatted as a journal article that has been submitted to a peer-reviewed journal. Because of the nature of peer-reviewed literature, the final version of this document will be modified based on reviewer comments and the specific formatting guidelines of the publishing journal. The final version of the paper will be submitted to the U.S. Department of Energy project manager.

References

Bennion, B., and Bachu, S., 2007, Permeability and relative permeability measurements at reservoir conditions for CO_2–water systems in ultralow-permeability confining caprocks: Paper presented at the EUROPEC/EAGE Annual Conference and Exhibition, London, England, SPE-106995-MS.

Bennion, B., and Bachu, S., 2005, Relative permeability characteristics for supercritical CO_2 displacing water in a variety of potential sequestration zones: Paper presented at the SPE Annual Technical Conference and Exhibition, Dallas, Texas, SPE-95547-MS.

U.S. Environmental Protection Agency, 2018, Underground Injection Control (UIC) Program Class VI implementation manual for UIC program directors, January 2018–2020: www.epa.gov/sites/default/files/2018-01/documents/implementation_manual_508_010318.pdf (accessed July 2022).

APPENDIX A

IMPACTS OF LOCAL GRID REFINEMENT (LGR), CAPILLARY PRESSURE, AND RELATIVE PERMEABILITY ON EARLY INJECTION WELL BEHAVIOR DURING SIMULATION OF LARGE-DOMAIN DEDICATED CARBON DIOXIDE STORAGE

IMPACTS OF LOCAL GRID REFINEMENT (LGR), CAPILLARY PRESSURE, AND RELATIVE PERMEABILITY ON EARLY INJECTION WELL BEHAVIOR DURING SIMULATION OF LARGE-DOMAIN DEDICATED CARBON DIOXIDE STORAGE

Thomas P. McGuire[a,b*], Dominic Druke[b], Stephen N. Guillot[b], Merry D. Tesfu[b], Todd Jiang[b], Chantsalmaa Dalkhaa[b], Matthew L. Belobraydic[b], and Nicholas W. Bosshart[b]

[a] National Energy Technology Laboratory (NETL)

[b] Energy & Environmental Research Center, University of North Dakota

*Corresponding Author Email: thmcguire@undeerc.org
Phone: (701) 777-5247; Fax: (701) 777-5181
Email: ddruke@undeerc.org
Email: sguillot@undeerc.org
Email: mtesfu@undeerc.org
Email: tjiang@undeerc.org
Email: cdalkhaa@undeerc.org
Email: mbelobraydic@undeerc.org
Email: nbosshart@undeerc.org

ABSTRACT

Results of large-domain carbon storage reservoir simulations conducted using a square grid initially showed early injection well pressure and rate trends inconsistent with typical CO_2, water, and gas injection well behavior measured in the field. To determine the potential cause of these differences, this simulation study was conducted to evaluate and quantify the relative effects of local grid refinement (LGR), relative permeability, and capillary pressure on long-term CO_2 injection well behavior. A large-domain (888-square mile) model of the Deadwood Formation (informally referred to as the Basal Cambrian) in the Williston Basin was used to simulate a single CO_2 injection well at two bottomhole injection pressures (BHIPs) with three different water–CO_2 relative permeability curves, both with and without capillary pressure. Without proper LGR, 12-year cumulative injected CO_2 mass is underpredicted by approximately 88% at a 90% fracture gradient BHIP. Reducing the BHIP requires smaller LGR cells to simulate expected early injection well behavior and indicates the need to review LGR for every realization of CO_2 injection, even after only changing BHIP or injection rate constraints. Error from excluding capillary pressure is observed to increase 12-year cumulative injection by 10% at a 90% fracture gradient BHIP and increases to 26% at the reduced BHIP. Finally, this study shows that relative permeability characterized by Bennion and Bachu,[1,2] provides similar simulation results compared to site-specific data at both explored BHIPs; therefore, these data can be temporarily used in place of site-specific data to accelerate the simulation-predicted CO_2 storage resource and injection rates.

Keywords: Carbon Storage, Capillary Pressure, CCS, CCS Simulation, Cell Size, Grid Size, LGR, Local Grid Refinement, PCOR, Relative Permeability, Simulation Grid, SMART

[1] Bennion, B., and Bachu, S., 2007, Permeability and relative permeability measurements at reservoir conditions for CO_2–water systems in ultralow-permeability confining caprocks: Paper presented at the EUROPEC/EAGE Annual Conference and Exhibition, London, United Kingdom.

[2] Bennion, B., and Bachu, S., 2005, Relative permeability characteristics for supercritical CO_2 displacing water in a variety of potential sequestration zones: Paper presented at the SPE Annual Technical Conference and Exhibition, Dallas, Texas.

3.0 INTRODUCTION

Reservoir simulation plays a critical role in planning industrial subsurface injection and production operations. While extensive work has been conducted to determine the optimum areal grid size to accurately represent various geologic depositional environments (fluvial, deltaic, etc.), significantly less guidance has been developed on how to simulate fluid flow with accurate near-wellbore effects while minimizing computational resources with an upscaled geologic model. Another key parameter in reservoir simulation that determines changes in fluid flow and displacement processes through time is relative permeability. The cause of unusual injection well behavior in a carbon capture and storage (CCS) reservoir simulation can be difficult to deconvolute without detailed analysis, since both simulation resolution and relative permeability can affect the evolution of fluid injection, displacement, and production. Therefore, after unusual transient injection well behavior was observed during CCS reservoir simulation, a study was conducted to determine the precise cause and recommend best practices for future CCS simulations. This type of sensitivity study was recommended by the "Plains CO_2 Reduction (PCOR) Partnership: Best Practices for the Technical Assessment of Geologic CO_2 Storage" as well as the "Plains CO_2 Reduction (PCOR) Partnership: Best Practices for Modeling and Simulation of CO_2 Storage" because of previously observed decreased injectivity with larger simulation grid cells (Wildgust and others, 2018; Bosshart and others, 2018). Capillary pressure effects were also included in the analysis because of their direct effects on relative permeability in fluid flow simulations.

Oil production operations have long recognized that increasing the resolution of reservoir simulations (smaller grid cell dimensions) can increase the accuracy of the fluid injection, displacement, or production predictions (Dogru and others, 2008). It is important to understand the range of grid cell sizes (resolution) and measured relative permeability data available that may be used in the absence of site-specific data.

Compositional and black oil are the two main types of reservoir simulations for oil and gas reservoirs. Black oil simulations can contain greater numbers of grid cells (higher resolution) compared to compositional simulations because compositional simulations are much more computationally intensive (require a greater number of unknown variables to be solved for in each cell at each time step) (Dogru and others, 2011). One of the largest oil and gas reservoir simulations, containing over 1 billion cells, is a black oil simulation with X and Y areal grid cell dimensions of 137 feet (Dogru and others, 2011). However, carbon dioxide (CO_2) storage reservoirs require compositional simulations for accurate realizations, so the compositional simulation of millions to billions of small simulation grid cells is not reasonable in most cases. Oil and gas research related to the effects of grid cell sizes in compositional modeling showed minimal effects at areal cell dimensions of 200 feet or less (Lim and others, 1997). Full-field compositional simulations for North America's largest oil field, Prudhoe Bay, used an areal grid cell dimension of 467 feet (Ding and others, 2009). The largest grid cells found being used in oil and gas simulations have areal dimensions of 656 feet (Samantray and others, 2003).

Simulations for CO_2 storage include both simulations with and without the use of local grid cell refinement (LGR) near features of interest. Most studies discussing horizontal grid cell dimensions of CO_2 injection and storage simulations without any type of LGR used cells between 131 and 328 feet (Cavanagh, 2013; Nilsen and others, 2011; Qi and others, 2009). CCS simulations with LGR can have grid cells with areal dimensions that are up to 3,280 feet in the "far field" (far from

simulation features of interest), with smaller elements refined to between 33 and 262 feet near simulation features of interest, such as wells or faults (Pruess and Nordbotten, 2011; Rohmer and others, 2013; Senel and Chugunov, 2013). Including both the oil and gas and carbon storage grid cell sizes, the largest areal grid cell size used near features of interest is 656 feet, but the approximate mean areal grid cell size used near features of interest is 212 feet. Therefore, this research simulates LGR that spans the mean areal grid size from this review near features of interest to understand the sensitivity and provide guidance for LGR of CO_2 storage simulations.

In addition to LGR, this research compares 12-year injection rates and behaviors of simulations both with and without capillary pressure and using site-specific relative permeability curves compared to relative permeability curves available from literature. Analysis was limited to a single injection well to avoid possible well interference effects. Relative permeability and capillary pressure curves from Bennion and Bachu's (2005, 2007) measurements are used as benchmark settings for the simulations.

For this study, the expected injection rate behavior of a CO_2 injection well constrained by a maximum bottomhole injection pressure (BHIP) is defined using an analog of gas injection into an oil and gas reservoir. Previous studies of gas injectivity show gas injection, at a set target rate, experiences increasing BHIP in the absence of thermal or other fracturing effects (Xu and others, 2020). This implies that injection rate would decrease through time when a maximum permitted BHIP constraint is reached. Water injectivity tests show the same type of response as gas injection wells (Earlougher, 1977).

2.0 GEOLOGIC MODEL DESCRIPTION AND ASSUMPTIONS

CO_2 storage predictive simulations are required to properly plan safe and economical injection and storage strategies. To predict performance and pressure plume development of prospective carbon storage projects in the Deadwood Formation (informally referred to as the Basal Cambrian (LeFever and others, 1987), a large-domain simulation model of the Basal Cambrian was created with a total areal dimension of approximately 30 miles by 30 miles with 1,500-foot X and Y grid cell dimensions. Cell thickness (Z-dimension) varied depending on the local reservoir thickness and whether cells represented reservoir or confining rock types with smaller vertical cell dimensions to better represent the vertical heterogeneity in reservoir rock. The model average thickness of each cell was approximately 16 feet while ranging in thickness from 0 to 73 feet. The number of grid cells in the X, Y, and Z directions were 105, 105, and 41, respectively, resulting in a total of 452,025 grid cells (shown in Figure 1). Table 1 provides more details of the simulation property values, such as average permeability and porosity for each zone in the simulation domain.

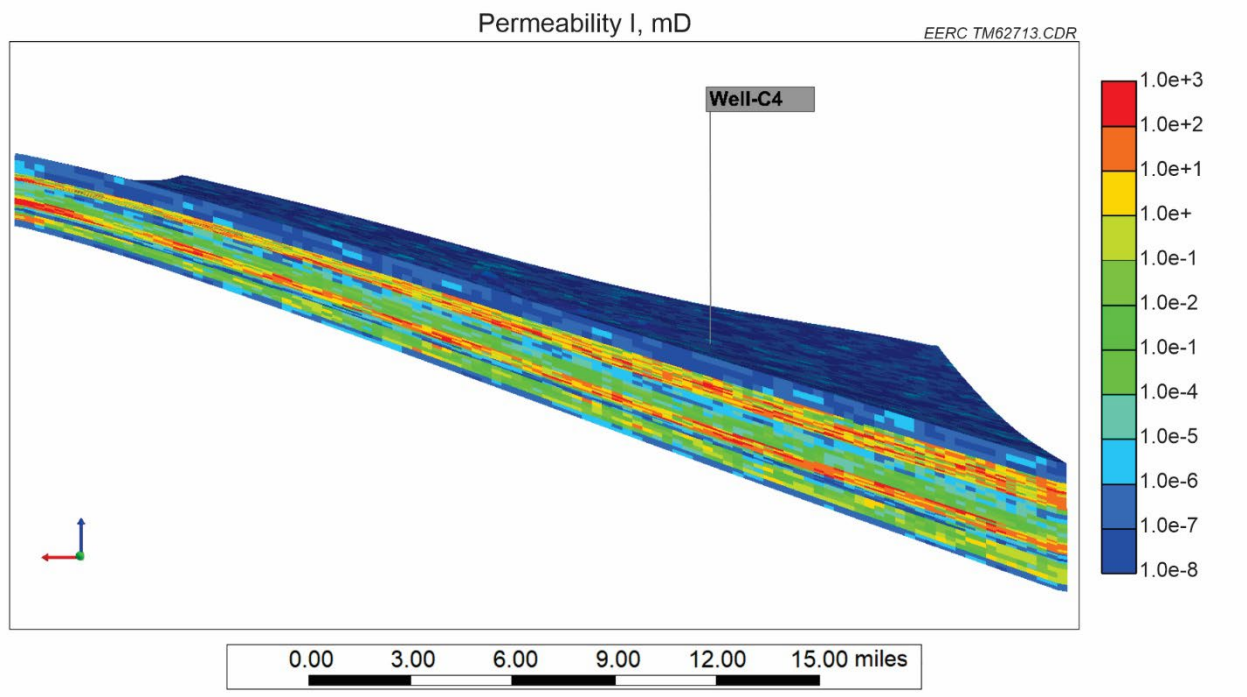

Figure 1. Simulation grid showing the horizontal permeability. Yellow, orange, and red indicate higher-permeability reservoir rock, while green and blue indicate lower-permeability intervals.

Table 1. Geologic Model Properties

Simulation Properties	Value
Number of Grid Cells (X, Y, Z)	105, 105, 41
Simulation Domain X and Y Dimension, miles	29.8
Vertical Permeability/Horizontal Permeability	0.05
Roughlock and Ice Box Formations	
Total Block Volume, ft^3	1.76E+13
Block Volume Weighted Average Horizontal Permeability, mD	3.68E-07
Block Volume Weighted Average Porosity	0.0012
Black Island Formation	
Total Block Volume, ft^3	4.50E+12
Block Volume Weighted Average Horizontal Permeability, mD	8.23
Block Volume Weighted Average Porosity	0.1171
Deadwood Formation – E Member	
Total Block Volume (ft^3)	9.02E+12
Block Volume Weighted Average Horizontal Permeability, mD	58.79
Block Volume Weighted Average Porosity	0.1127
Deadwood Formation – D Member	
Total Block Volume, ft^3	8.41E+12
Block Volume Weighted Average Horizontal Permeability, mD	2.26E-05
Block Volume Weighted Average Porosity	0.0036
Deadwood Formation – C Member Carbonate	
Total Block Volume, ft^3	1.06E+13
Block Volume Weighted Average Horizontal Permeability, mD	0.0043
Block Volume Weighted Average Porosity	0.0116
Deadwood Formation – C Member Sandstone	
Total Block Volume, ft^3	7.79E+12
Block Volume Weighted Average Horizontal Permeability, mD	45.37
Block Volume Weighted Average Porosity	0.1188
Deadwood Formation – Upper B Member	
Total Block Volume, ft^3	2.19E+12
Block Volume Weighted Average Horizontal Permeability, mD	0.0047
Block Volume Weighted Average Porosity	0.0101
Deadwood Formation – B Member Shale	
Total Block Volume, ft^3	3.87E+12
Block Volume Weighted Average Horizontal Permeability, mD	2.07E-05
Block Volume Weighted Average Porosity	0.0013
Deadwood Formation – Lower B Member and A Member	
Total Block Volume, ft^3	9.53E+12
Block Volume Weighted Average Horizontal Permeability, mD	0.9803
Block Volume Weighted Average Porosity	0.0397
Precambrian Basement	
Total Block Volume, ft^3	5.87E+12
Block Volume Weighted Average Horizontal Permeability, mD	6.06E-07
Block Volume Weighted Average Porosity	0.0074

The geomodel was built to support the dynamic simulation of the CO_2 plume and the associated pressure elevation for planned injection into the high-porosity and permeability sandstone units of the Deadwood Formation. Using the lithostratigraphic correlation scheme proposed in LeFever and others (1987), the structural grid and property model were constructed using well wireline logs for 13 wells, core sample data, and seismic data.

The Deadwood Formation unconformably overlies the Precambrian granitic basement and was deposited as three sequences of offshore marine, marginal marine, and carbonate buildups associated with transgressive and regressive cycles over late Cambrian and early Ordovician time (LeFever and others, 1987). At the area of interest, not disclosed in this paper because of sensitivities around a future potential commercial CCS operation, all Deadwood lithostratigraphic members are present except the F member, which is not present because of an erosional unconformity. The late Ordovician Winnipeg Group unconformably overlies the Deadwood Formation with nearshore and deltaic sands of the Black Island Formation, followed by the offshore marine shales of the Icebox Formation and limestone of the Roughlock Formation (LeFever and others, 1987) (Figure 2).

Porosity and permeability were distributed through collocated co-simulation property trends. The final grid and property volumes were upscaled to ensure cell count reductions and geologic conceptual model preservation to the grid dimensions described previously.

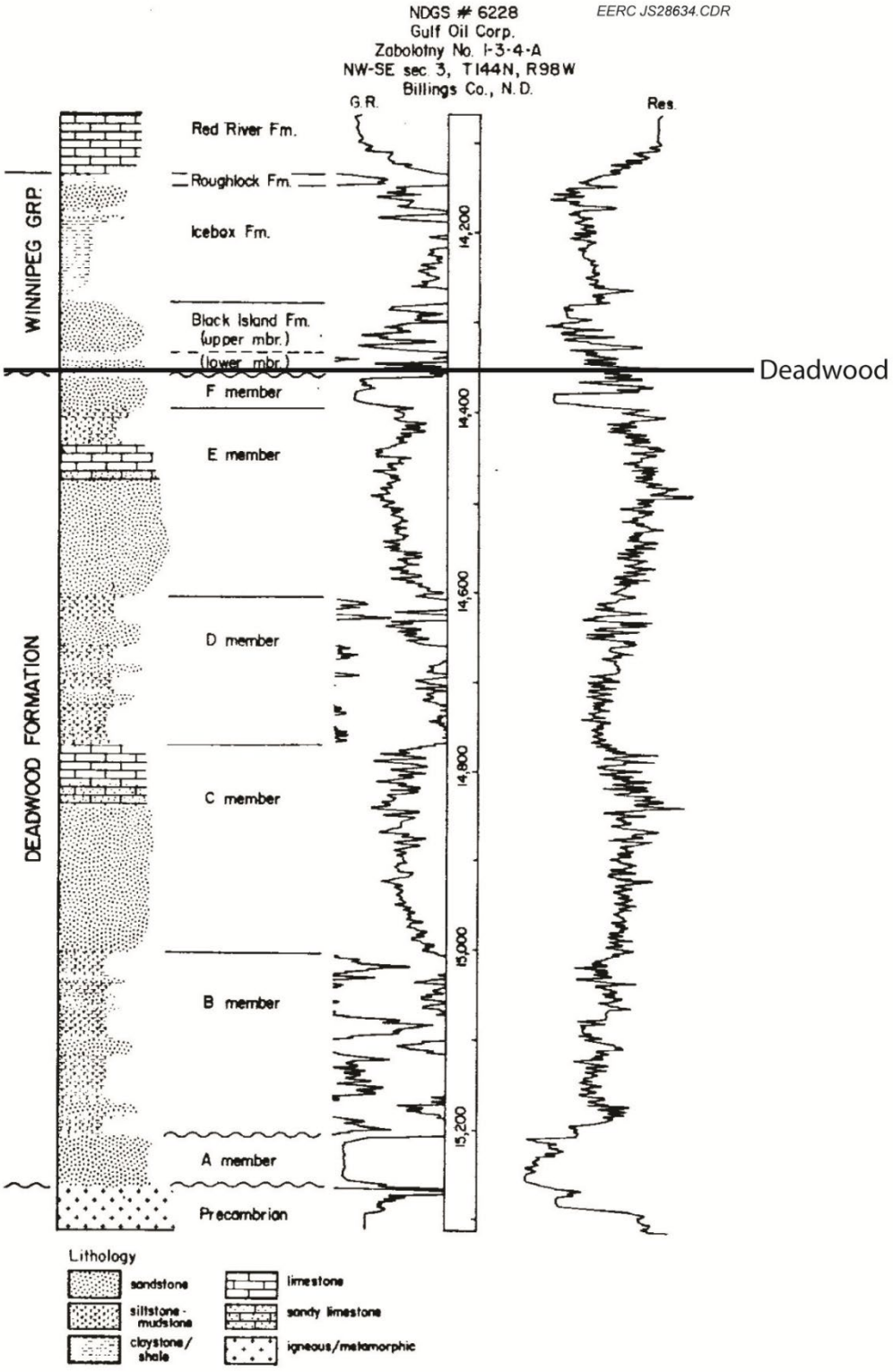

Figure 2. Stratigraphic column of the Deadwood Formation and Winnipeg Group, with representative well log responses after LeFever and others (1987).

3.0 SIMULATION DESCRIPTION AND ASSUMPTIONS

Reservoir simulations were conducted using Computer Modeling Group's (CMG's) 2019 Generalized Equation-of-State Model (GEM) compositional simulation software. Open lateral reservoir boundaries were assumed because of the continuity of the Basal Cambrian sandstone in the Williston Basin by applying a volume modification multiplier of 100 around the perimeter of the simulation domain. The volume modification multiplier allowed the simulated pressure and injection response to be similar to a storage formation with continuous hydraulic communication that extends significantly beyond the simulation domain in all directions. The resulting infinite-acting aquifer leads to the single well injection rate falling from the start of injection and reaching a steady-state rate of injection at a given BHIP. In these simulations, steady-state injection rates are observed within the first 3 years of injection in most cases, with subsequent years showing a continued constant injection rate at a fixed BHIP.

The depth of the top perforation of the one well in the simulation was 10,052 feet true vertical depth from the surface in a vertical well configuration. The only constraint for injection in the simulations was BHIP. Depending on the simulation case, it was set to either a maximum of 90% of the fracture gradient to comply with the U.S. Environmental Protection Agency underground injection control (UIC) Class VI (dedicated CO_2 injection) well regulatory constraints (equal to 5,931 psi), or a reduced BHIP of 5,080 psi, to explore the sensitivity of the LGR, capillary pressure, and relative permeability to injection pressure (U.S. Environmental Protection Agency, 2018). Previous publications characterize the bottomhole fracture pressure gradient of the Basal Cambrian to be 14.9 kPa/m (0.66 psi/ft), which infers a bottomhole fracture propagation pressure at 10,052 feet in this study of 6,634 psi (Stork and others, 2018). 90% of this fracture propagation gradient is 0.59 psi/ft, correlating to a maximum UIC Class VI BHIP of 5,931 psi. Other reservoir parameters included an initial reservoir pressure and temperature of 4,740 psi and 83°C (181°F) and reservoir brine total dissolved solids of 256,000 ppm.

To match CO_2 capture rates from CCS projects, it is common to also set an injection rate limit in CCS simulations. However, early CCS industry partners and investors in the United States are currently seeking to maximize the utility and return on their investments, including CO_2 injection wells. Therefore, many are seeking additional sources of CO_2 to inject higher rates of CO_2 at the start of injection when it is possible without exceeding EPA Class VI injection regulations. These higher early rates provide a more rapid and certain return on investment compared to cases where injectivity is not maximized and call for this research on reservoir simulation to best discern the higher injectivity in early CO_2 injection well behavior.

LGR was necessary to increase the resolution from the 1,500-foot grid cells of the unrefined model to observe expected early injection well behaviors. To test the effects of local grid size on predicted CO_2 injection and storage, the grid cells containing the injection well were horizontally refined into 3 × 3, 5 × 5, 7 × 7, 9 × 9, and 11 × 11 grid cells, resulting in grid cells with areal dimensions as small as 136 feet. The benchmark case, for comparison with all others, had relative permeability data from Bennion and Bachu (2007, 2005), did not use LGR (1500-foot grid cells), and included capillary pressure (Case 1). Additional simulations were run to discern the relative effects of the LGR region size as well as the BHIP.

Careful consideration was given when deciding on the duration of injection to simulate since some existing CCS projects have been injecting for over 20 years. However, since current U.S. federal law only provides tax credits for 12 years of CO_2 storage, it was decided to run 12-year simulations consistent with the duration of tax credits that current industry projects can expect with reasonable certainty (Internal Revenue Service, 2020). If an industry partner is unable to realize a return on their investment within the 12 years of current tax credit eligibility, the project is not expected to move forward with industry investors at the current time within the United States. As experience and technology for CCS grow or if 45Q tax credit duration increases, projects with longer injection duration and payback periods are expected to become more common. But for this research, it was desired to discern early injector behavior effects of LGR, capillary pressure, and relative permeability that are important in current CCS projects in the United States. All simulations assumed an adaptive time step simulation control. The resulting matrix of simulations is described in Table 2. Well cell X–Y dimensions refers to the X–Y dimensions of the refined cells within the LGR region near the injection well. Outside of the LGR region, simulation cells were 1,500 feet in all simulations.

Table 2. Scenarios for Comparison of Predicted CCS Injection

Case	Capillary Pressure	LGR	LGR Region Radius, ft	Relative Permeability	Well Cell X–Y Dimension, ft	BHP Injection Pressure, psi
1, 2	On, off	None	750	Bennion and Bachu	1,500	5,931
3, 4	On, off	3 × 3	750	Bennion and Bachu	500	5,931
5, 6	On, off	5 × 5	750	Bennion and Bachu	300	5,931
7, 8	On, off	7 × 7	750	Bennion and Bachu	214	5,931
9, 10	On, off	9 × 9	750	Bennion and Bachu	167	5,931
11, 12	On, off	11 × 11	750	Bennion and Bachu	136	5,931
13, 14	On, off	None	750	Linear S_w end points 0–100%	1,500	5,931
15, 16	On, off	3 × 3	750	Linear S_w end points 0–100%	500	5,931
17, 18	On, off	5 × 5	750	Linear S_w end points 0–100%	300	5,931
19, 20	On, off	7 × 7	750	Linear S_w end points 0–100%	214	5,931
21, 22	On, off	9 × 9	750	Linear S_w end points 0–100%	167	5,931
23, 24	On, off	11 × 11	750	Linear S_w end points 0–100%	136	5,931
25, 26	On, off	None	750	Site-specific	1,500	5,931
27, 28	On, off	3 × 3	750	Site-specific	500	5,931
29, 30	On, off	5 × 5	750	Site-specific	300	5,931
31, 32	On, off	7 × 7	750	Site-specific	214	5,931
33, 34	On, off	9 × 9	750	Site-specific	167	5,931
35, 36	On, off	11 × 11	750	Site-specific	136	5,931
37, 38	On, off	7 × 7	2,250	Bennion and Bachu	214	5,931
38, 40	On, off	7 × 7	3,750	Bennion and Bachu	214	5,931

Continued . . .

Table 2. Scenarios for Comparison of Predicted CCS Injection (continued)

Case	Capillary Pressure	LGR	LGR Region Radius, ft	Relative Permeability	Well Cell X–Y Dimension, ft	BHP Injection Pressure, psi
41, 42	On, off	7 × 7	5,250	Bennion and Bachu	214	5,931
43, 44	On, off	7 × 7	2,250	Linear S_w end points 0–100%	214	5,931
45, 46	On, off	7 × 7	3,750	Linear S_w end points 0–100%	214	5,931
47, 48	On, off	7 × 7	5,250	Linear S_w end points 0–100%	214	5,931
49, 50	On, off	11 × 11	2,250	Site-specific	136	5,931
51, 52	On, off	11 × 11	3,750	Site-specific	136	5,931
53, 54	On, off	11 × 11	5,250	Site-specific	136	5,931
55, 56	On, off	None	750	Bennion and Bachu	1,500	5,080
57, 58	On, off	3 × 3	750	Bennion and Bachu	500	5,080
59, 60	On, off	11 × 11	750	Bennion and Bachu	136	5,080
61, 62	On, off	13 × 13	750	Bennion and Bachu	115	5,080
63, 64	On, off	15 × 15	750	Bennion and Bachu	100	5,080
65, 66	On, off	17 × 17	750	Bennion and Bachu	88	5,080
67, 68	On, off	19 × 19	750	Bennion and Bachu	79	5,080
69, 70	On, off	21 × 21	750	Bennion and Bachu	71	5,080
71, 72	On, off	15 × 15	2,250	Bennion and Bachu	100	5,080
73, 74	On, off	15 × 15	3,750	Bennion and Bachu	100	5,080
75	On	None	750	Linear S_w end points 0–100%	1,500	5,080
76	On	3 × 3	750	Linear S_w end points 0–100%	500	5,080
77	On	11 × 11	750	Linear S_w end points 0–100%	136	5,080
78	On	13 × 13	750	Linear S_w end points 0–100%	115	5,080
79	On	15 × 15	750	Linear S_w end points 0–100%	100	5,080
80	On	15 × 15	2,250	Linear S_w end points 0–100%	100	5,080
81	On	15 × 15	3,750	Linear S_w end points 0–100%	100	5,080
82	On	None	750	Site-specific	1,500	5,080
83	On	3 × 3	750	Site-specific	500	5,080
84	On	11 × 11	750	Site-specific	136	5,080
85	On	13 × 13	750	Site-specific	115	5,080
86	On	15 × 15	750	Site-specific	100	5,080
87	On	15 × 15	2,250	Site-specific	100	5,080
88	On	15 × 15	3,750	Site-specific	100	5,080

Three different sets of relative permeability data were tested for the storage formation. The default relative permeability curves for the simulations used the Basal Cambrian sandstone and Wabamun low-permeability carbonate from Bennion and Bachu (2005) and the Colorado Group Shale from Bennion and Bachu (2007) (Figure 3). To test the impact of different relative permeability curves, results using the data of Bennion and Bachu (2005, 2007) were compared with both a set of site-specific relative permeability curves measured in a carbon storage project in the PCOR Partnership region, shown in Figure 4, and a set of linear relative permeability curves with water saturation end points of 0% and 100% to represent an extremely different relative permeability, shown in Figure 5. All three sets of relative permeability curves used the same capillary pressure versus water saturation curves, shown in Figure 6, for consistency. Simulations were also run without accounting for the effects of capillary pressure to discern the relative importance of capillary pressure on injection rates.

Numerical settings in the simulations were set to internally adjust the time step size such that the target average change in pressure, saturation, global mole fraction, and change in aqueous reactions during a time step equals approximately 2000 psi, 0.15, 0.1, and 0.3, respectively. Finally, simulations were all run using 16 parallel computing cores.

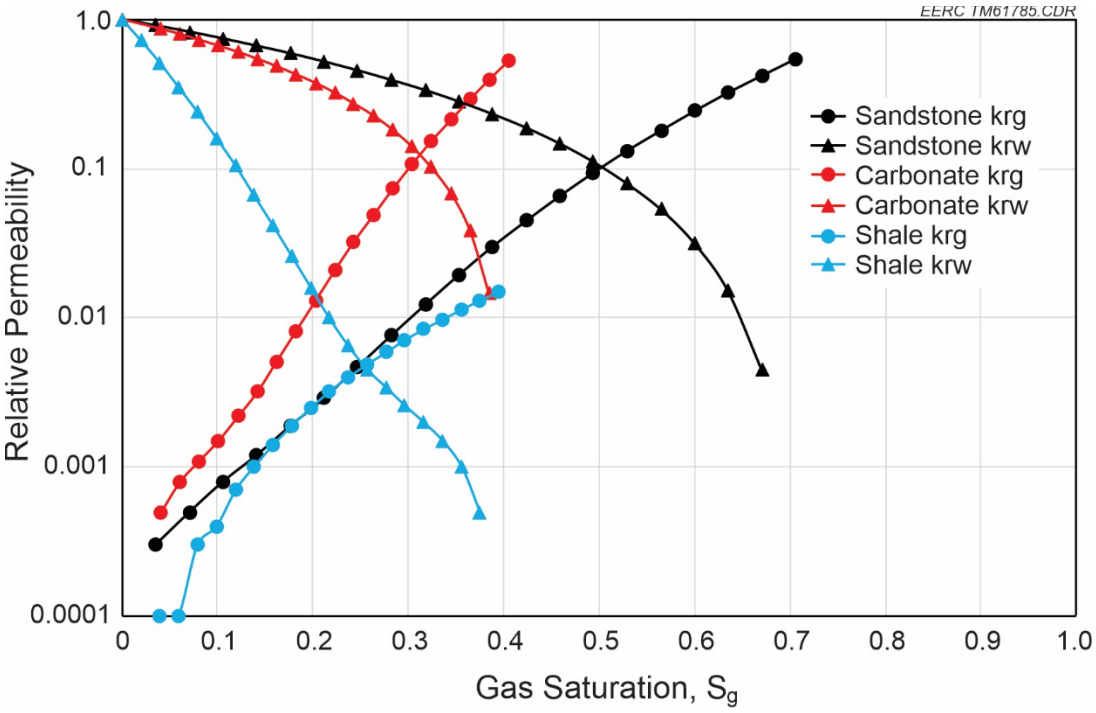

Figure 3. Bennion and Bachu (2005, 2007) Basal Cambrian sandstone, Wabamun carbonate, and Colorado Group shale relative permeability curves.

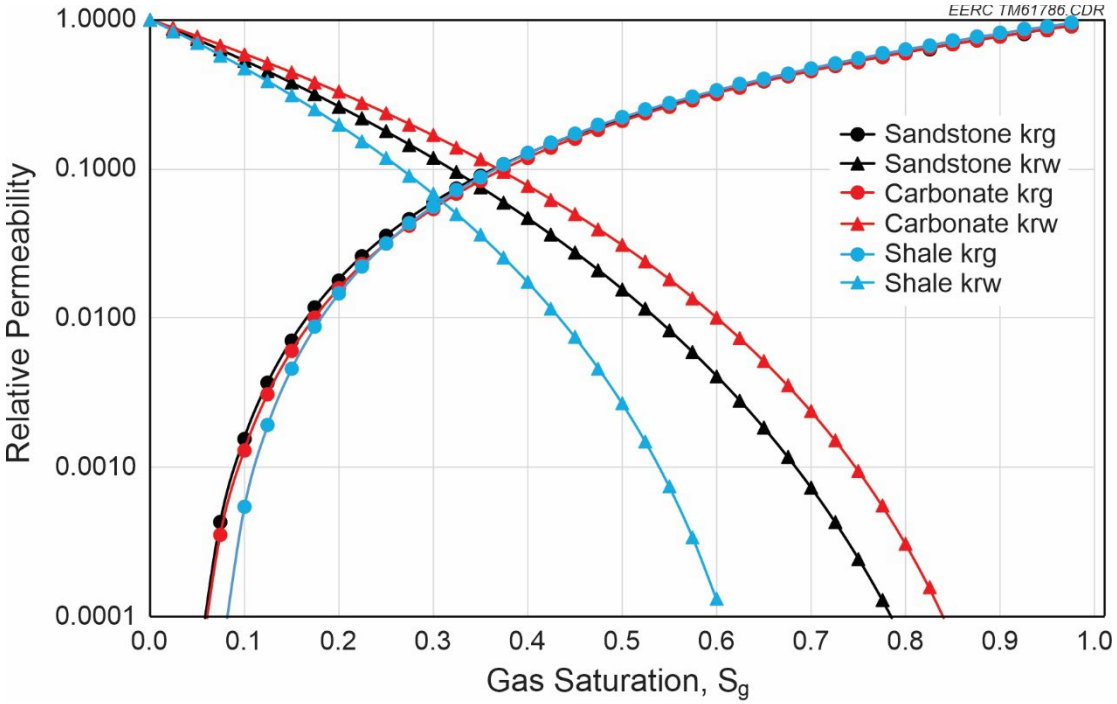

Figure 4. Site-specific Deadwood Formation relative permeability curves.

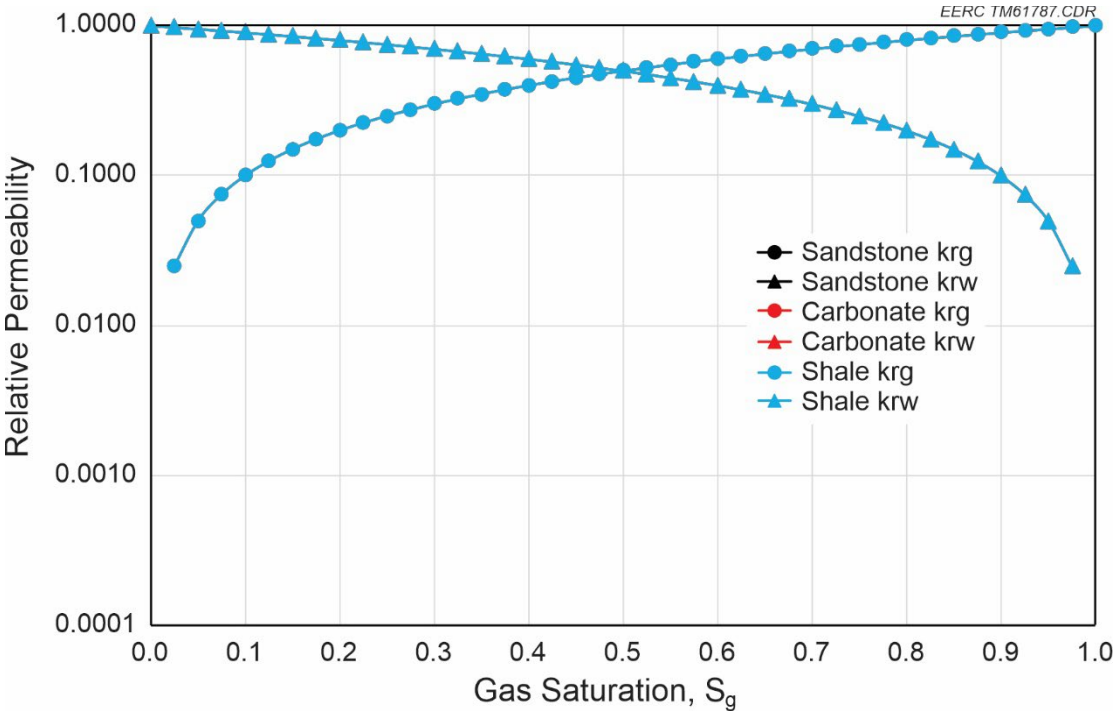

Figure 5. Linear relative permeability curves with water saturation (S_w) end points of 0–100%.

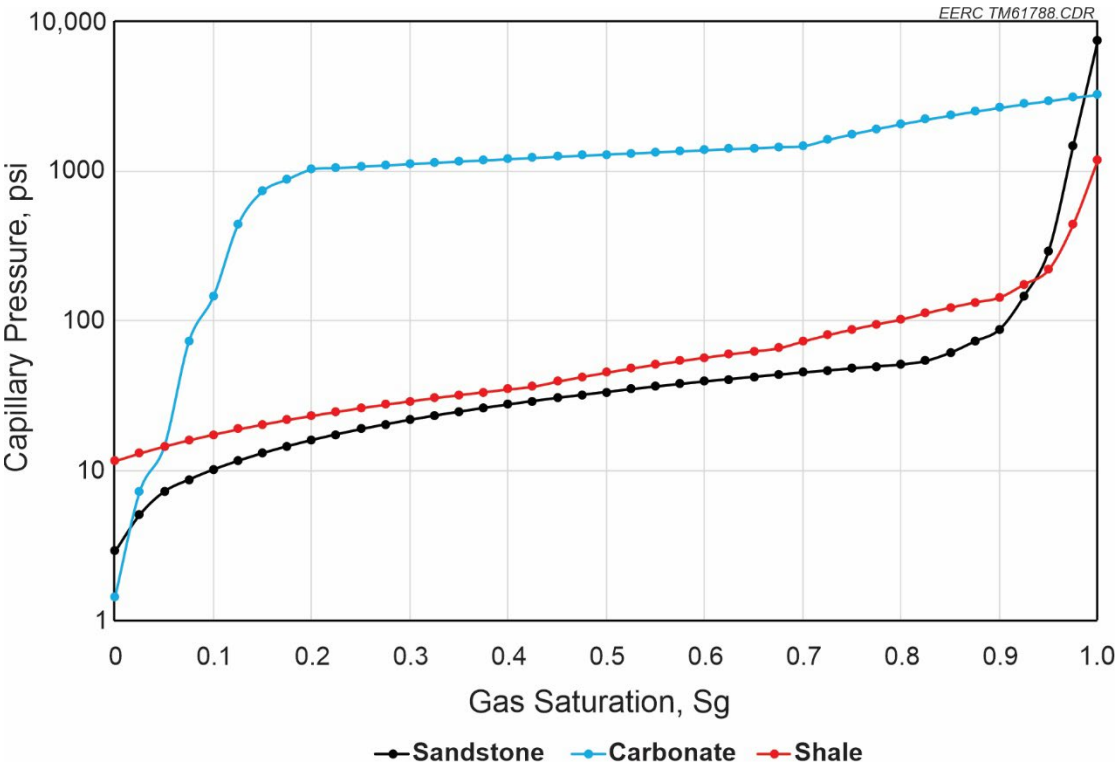

Figure 6. Bennion and Bachu (2005, 2007) Basal Cambrian sandstone, Wabamun carbonate, and Colorado Group shale capillary pressure curves.

4.0 RESULTS AND DISCUSSION

Simulation Results and Data

To compare the accuracy and consistency of the simulations, the cumulative injected CO_2 volume of each case was compared to Case 1 (benchmark case). The long-term injection rate trends of each case were also compared to the expected injection well behavior (decreasing injection rate through time at a fixed BHIP). The results, in percent difference of the cumulative 12-year CO_2 injection from Case 1 calculated by equation 1 for Cases 1–36 versus the areal dimension of the grid cell containing the injection well, are shown in Figure 7. It shows the relationship between the cell's X–Y dimension and percent change in the 12-year cumulative CO_2 injected, supporting the inference that injectivity decreases as simulation areal cell size increases, as shown previously in the "Plains CO_2 Reduction (PCOR) Partnership: Best Practices for Modeling and Simulation of CO_2 Storage" (Bosshart and others, 2018). Additionally, these results show that unrefined grid cells can have a similar magnitude of effect on predicted cumulative CO_2 injection compared to using linear relative permeability curves. Refining the grid cells of the parent well cell to 136 feet resulted in an average increase in cumulative injection of 64%. Meanwhile, using linear relative permeability curves in place of more appropriate data from literature or site-specific data resulted in an average increase of 79% in 12-year cumulative injection compared to the same case using Bennion and Bachu's (2005, 2007) relative permeability curves. All simulations except one had material balance errors of 1% or less.

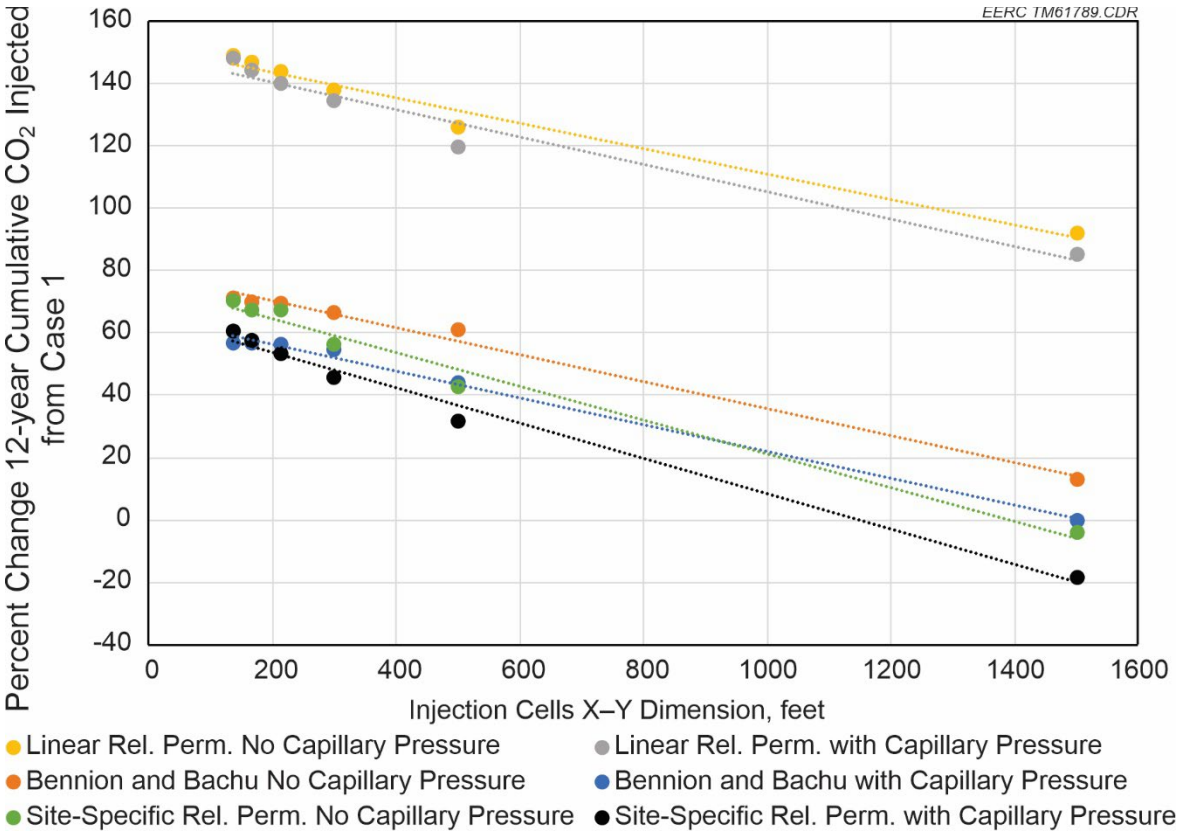

Figure 7. Percent change in 12-year cumulative injection of Cases 1–36 from benchmark Case 1.

Equation 1 $$\frac{100*(Case\ N - Case\ 1)}{Case\ 1}$$

As expected, when reviewing the injection rate trends in cases with refined cell areal dimensions of 136 feet or less, higher rates at the start of injection that decreased to a stabilized value by the end of the 12 years of injection were observed. In less refined simulations (larger cells around the well), the injection rate was observed to increase, not following expected injection well behavior, as seen from field data. Figure 8 shows these two different injection rate trends. Figure 8A shows typical injection well behavior, and Figure 8B shows atypical rate trends. Increasing injectivity was observed in unrefined simulations (rather than typical decreasing injectivity) due to the larger volume of the cells containing and surrounding the injection well. Greater amounts of injected CO_2 are required before CO_2 saturations increase enough to significantly increase the relative permeability to CO_2. Smaller, more refined cells decrease volume of CO_2 required to increase the CO_2 saturation, decreasing the time required to reach nearly stabilized well cell transmissibility from a timescale of years to months or days.

Figure 8. A) Expected (generally decreasing rate) injection well behavior with refined grid cells and B) nontypical (increasing rate) injection well behavior with unrefined well cells.

Simulations were also tested for effects of an LGR radius from the well. Including the injection well location, nine-cell (3 × 3), 25-cell (5 × 5), and 49-cell (7 × 7) LGR regions (radii of 2,250, 3,750, and 5,250 feet, respectively) were tested for their effects on simulated injection rates and cumulative injected CO_2. Table 2 shows the simulation matrix for these expanded LGR areas as Cases 37–54. In the cases of Bennion and Bachu's relative permeability and linear relative permeability curves with end point water saturations of 0%–100%, refined cells could be up to 214 feet while still showing expected injection well behavior (decreasing injection rate through time at a fixed BHIP) (Bennion and Bachu, 2005, 2007). Therefore, the LGR region size sensitivity was conducted with 214-foot refined grid cells for those two relative permeability curve inputs (both with and without capillary pressure). LGR region size sensitivity was conducted using 136-foot grid cells for the proprietary site-specific data since that was the largest local grid size that resulted in expected injection well behavior.

Decreasing the injection rate required the LGR to increase to a 15 × 15 cell refinement (X–Y grid cell dimension of 100 feet) for expected injection well behavior. Decreasing the LGR cell size was needed at lower injection rates to simulate expected injector behavior because of lower injection rates requiring more time to reach a semi-steady-state CO_2 saturation, and thus relative permeability, near the well. Further decreasing the injection rate below rates used in this study while keeping all other assumptions constant would potentially require the LGR X–Y grid cell dimensions to be further reduced to less than 100 feet. As with the higher rate injection simulations, the 15 × 15 LGR region was expanded to 2,250 and 3,750-foot radii to measure the impact of increasing the LGR region size.

The computational penalty (increase in amount of time needed to run numerical simulations) for the increased accuracy of LGR will be represented by the number of increased cells compared to the unrefined simulation. Table 3 shows the calculated increase in the simulation cell count and percent increase in cells (and inferred computational intensity) over the benchmark case. Caution must be observed when simulating low rates of CO_2 injection that proper LGR cell sizes are utilized without increasing the computational intensity of simulations to unreasonable levels, especially when multiple injection wells are simulated and multiple LGR regions are required.

Table 3: Calculated Cell/Computational Intensity Increase of Simulations with LGR over the Benchmark Case

LGR	Radius of LGR Region, ft	Total Simulation Cells	Cell Count Increase Over Benchmark, %
None	N/A	452,025	0
3 × 3	750	452,353	0.1
5 × 5	750	453,009	0.2
7 × 7	750	453,993	0.4
9 × 9	750	455,305	0.7
11 × 11	750	456,945	1.1
13 × 13	750	458,913	1.5
15 × 15	750	461,209	2.0
17 × 17	750	463,833	2.6
19 × 19	750	466,785	3.3
21 × 21	750	470,065	4.0
7 × 7	2250	469,737	3.9
7 × 7	3750	501,225	10.9
7 × 7	5250	548,457	21.3
11 × 11	2250	496,305	9.8
11 × 11	3750	575,025	27.2
11 × 11	5250	693,105	53.3
15 × 15	2250	534,681	18.3
15 × 15	3750	681,625	50.8

A particularly important observation from the LGR region size sensitivity analysis is that the LGR region's size had a significant impact on the injection well's long-term stable injection rate. Early

injection rates increase significantly as the degree of refinement increases (decreasing X–Y LGR cell dimensions), but in most cases, the injectivity curves converge to the same rate within 2 years following injection initiation. This is because the relative permeability to CO_2 increases more rapidly near the well with decreasing LGR cell dimensions. Increasing the radius of the LGR region, meanwhile, significantly increases the long-term injection rate compared to parent well cell-only refinement. Mechanisms that lead to this observation are that long-term injectivity is affected by the semi-steady-state pressure elevation that develops near the well. A larger LGR region allows a smaller pressure drop to develop in the LGR region around the well, leading to a higher steady-state rate of injection. Therefore, it is important for accurate short- and long-term injection forecasting to refine with small enough cells to resolve short-term injectivity while also refining a large enough LGR region to accurately predict long-term injectivity. Figure 9A and Figure 9B show the changes in injection rate with respect to well cell size and LGR region radius, respectively.

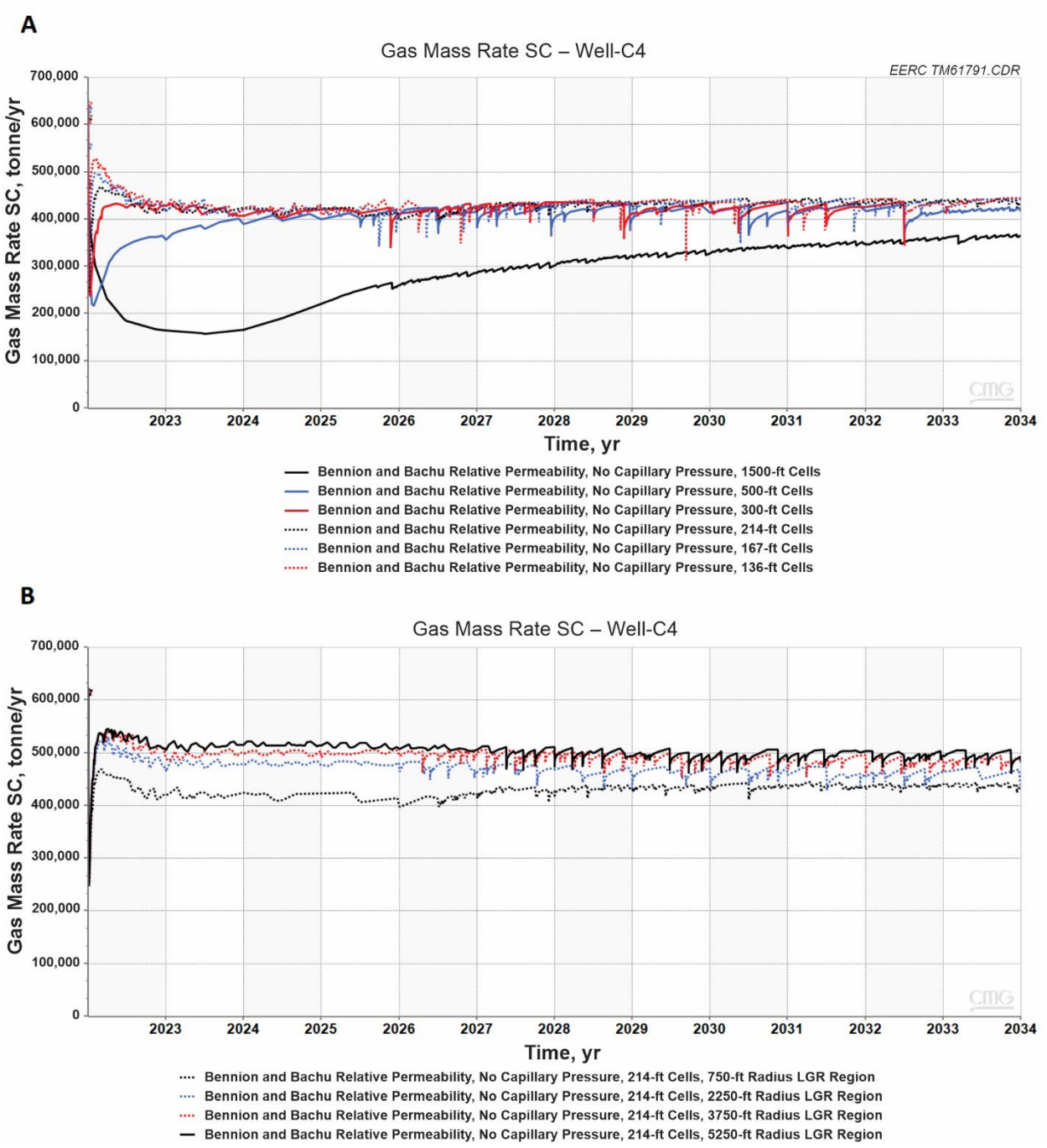

Figure 9. A) Increasing early injection rates with greater cell refinement (smaller cells) and B) increased long-term injection rates with a larger LGR region radius with the same LGR cell size.

Relative to Case 1, the cumulative injection is simulated to increase 90% or more with an LGR for parent cell regions of 5 × 5 and 7 × 7 (corresponding to regions with a radius of approximately 3,750 and 5,250 feet, respectively). However, LGR in these increasingly large regions begins to quickly increase the computational requirements, especially with the 11 × 11 LGR (136-ft cell size).

Fitting logarithmic curves to the observed data shows a consistent relationship between the expected 12-year cumulative injection with respect to the increase in the number of simulation grid cells. Additionally, it shows that the inclusion of capillary pressure effects is expected to decrease the 12-year cumulative CO_2 injection capacity by approximately 10% when injecting at 90% of the fracture gradient. These data and curve fits are shown in Figure 10.

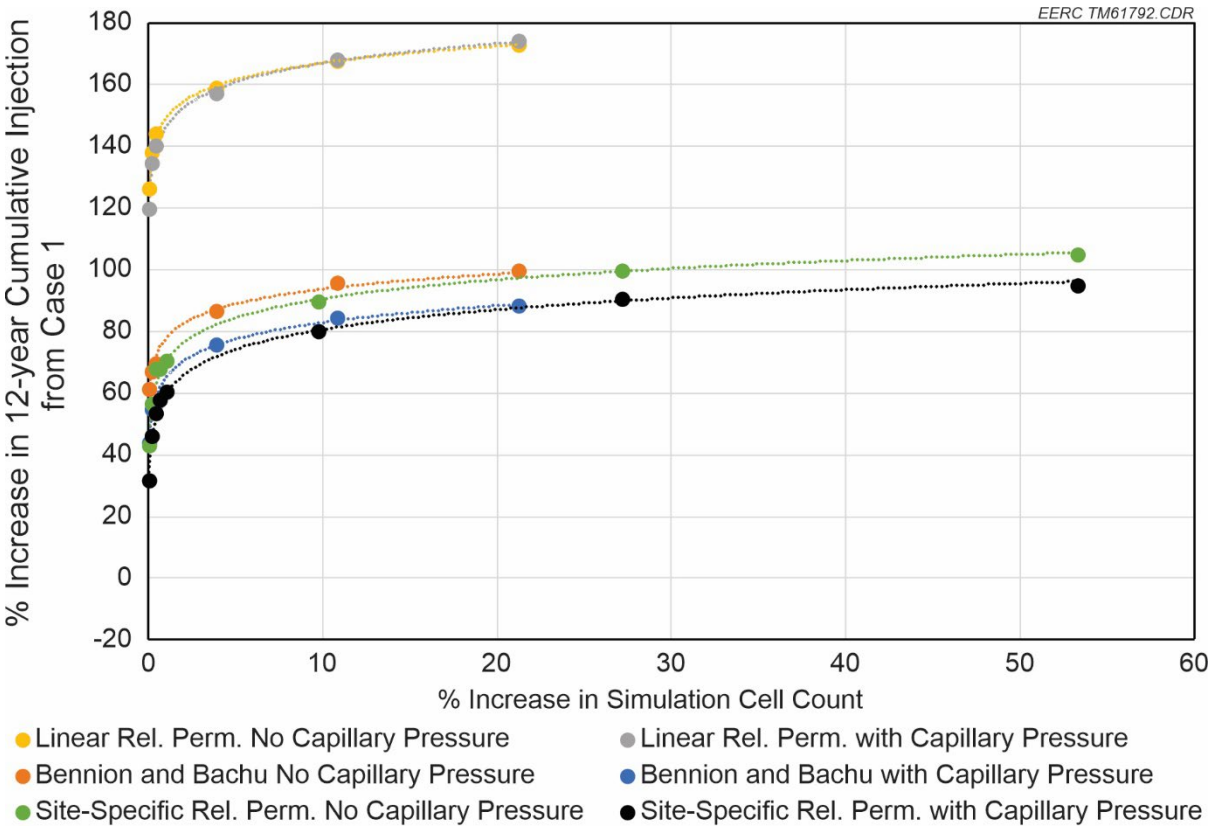

Figure 10. Log fits to predict changes of injection associated with further refinement and greater increase in simulation cell count.

At 90% fracture propagation pressure, 136-ft LGR cells with an LGR region radius of 3750 feet around the injection well are shown to nearly double the 12-year cumulative injection compared to benchmark Case 1. This LGR setting only increases the number of cells (and implied computational intensity) by 27% per injection well per LGR region.

At BHIPs significantly less than 90% fracture propagation pressure (resulting in injection rates equal to approximately 25% of maximum rate), LGR cells must decrease in X–Y dimensions to 100 feet or less to achieve expected CO_2 injection well behavior. However, the LGR region radius needed to remain constant at 3750 feet or more to avoid underpredicting the long-term injection rate. The computational intensity of these simulations increased by approximately 51% per well per LGR region beyond Case 55, which was the benchmark low-BHIP case. Figure 11 shows that low BHIP simulations showed nearly twice the error in the predicted 12-year cumulative CO_2 injection by using unrefined well cells compared to cases with a BHIP set at 90% of the fracture propagation pressure (Figure 10). This work only simulated one injection well. If multiple wells are used, then additional equal-sized and equally refined LGR regions would likely be needed around each additional well, so the cell count/computational intensity should increase by approximately the same amount per additional injection or production well.

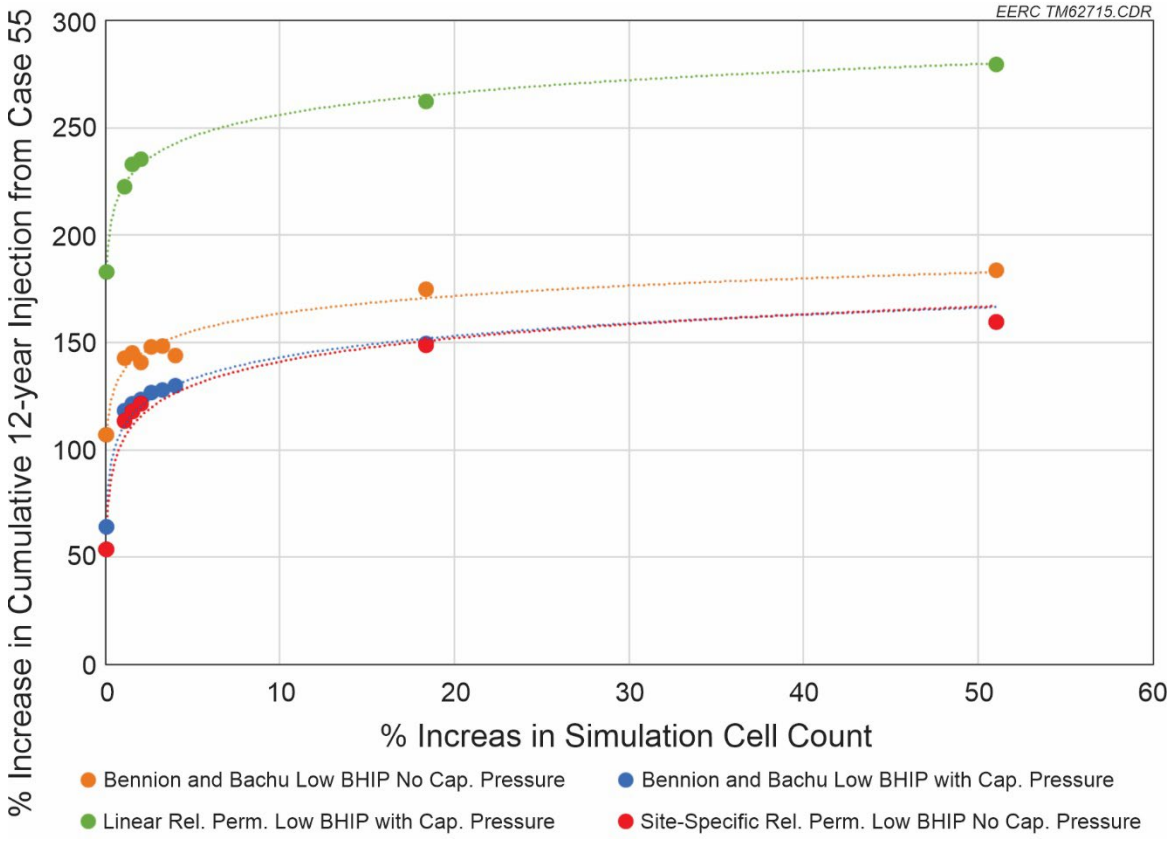

Figure 11. Increased sensitivity to LGR and capillary pressure at lower BHIP (Cases 55–88).

Refined low-BHIP cases measured a 160% increase in 12-year cumulative CO_2 injection over the unrefined low-injection-pressure case compared to only an 88% increase for cases injecting at high BHIP equal to 90% of the fracture propagation pressure. Likewise, low-BHIP cases measured a 26% decrease in a 12-year cumulative injection when adding capillary pressure effects compared to only a 10% decrease for cases injecting at a high BHIP (90% of fracture propagation pressure). This increased difference between cases with and without capillary pressure at lower injection

pressure occurs because lower injection pressures result in slower growth of CO_2 saturation and, therefore, do not allow the relative permeability to increase as much as those with higher injection pressures when the same capillary pressure curves are used. Low-BHIP cases with the linear relative permeability curves with 0%–100% end points and capillary pressure were measured to have a 280% increase in injectivity compared to the benchmark low-BHIP Bennion and Bachu case with capillary pressure. Comparable cases injecting at high BHIP, shown in Figure 10, only increase the 12-year cumulative injection by approximately 170%.

Significant Considerations Outside the Scope of This Study

This study focused specifically on the injection well behavior during short-term CO_2 injection in a saline sandstone formation. Two significant considerations beyond the injection well behavior are accurately simulating CO_2 dissolution during long-term storage and accurately representing the geologic system. Gorecki and others simulated 50–500 years of CO_2 injection and found that solubility trapping represented a significant portion of CO_2 storage over longer timeframes but also larger grid cells over-estimated solubility trapping effects (Gorecki and others, 2014). Therefore, if CO_2 dissolution and solubility trapping are expected to be an important mechanism, a similar sensitivity to the LGR cell size within the forecast CO_2 plume should be conducted.

Meanwhile, accurate representation of the geologic system and reservoir ideally requires the highest-resolution model and simulation possible to represent spatial distribution of reservoir properties. However, Bosshart and others reported that an X–Y cell size of up to 500 feet appropriately balanced the simulation run time with a reasonable representation of heterogeneity of the depositional environment (Bosshart and others, 2018).

Discussion

The paramount significance of this research is that it provides data to demonstrate that the necessary LGR for expected early CO_2 injection well behavior is dependent on the simulation BHIP constraint and, thus, indirectly dependent on the relative injection rate. Lower BHIP or injection rate constraints required smaller injection well cell X–Y dimensions to simulate expected early injection well behavior. This is a significant finding because it is not common practice to review the LGR grid cell size of a simulation due to changing the BHIP or injection rate constraints of an oil and gas simulation. This work demonstrates that reviewing a fit-for-purpose local grid refinement around injection wells and revising them to achieve expected early injection pressure and rate behavior is a significant additional simulation step that should be performed for every individual simulation in future suites of CO_2 injection simulations.

A similar dependency on the BHIP and injection rate was observed in the error caused by excluding the capillary pressure from the simulations with higher error at lower BHIPs and injection rates. However, one important finding to note is that even though the necessary LGR cell size changed depending on the BHIP or injection rate constraints of the simulation, the size of the LGR region did not have the same degree of dependency.

Finally, this work shows the amount of local grid refinement near injection wells necessary to accurately simulate CO_2 injection is higher than most previous oil and gas injection simulations. Some CO_2 injection cases in this research required the well cell X–Y dimensions to be reduced to as little as 30 meters before expected injection well behavior was observed. Meanwhile, a review

of oil and gas reservoir simulation LGR cell sizes near features of interest found in literature almost always exceeded 40 meters. This increased sensitivity of CO_2 injection simulations to LGR compared to typical oil and gas simulations explains why early simulations showed unexpected injection well behavior despite following typical oil and gas LGR guidance.

5.0 CONCLUSIONS

Based on observations of unusual injection well behavior in Basal Cambrian carbon storage reservoir simulations for a project in the PCOR Partnership region, a sensitivity study was conducted on the relative effects of LGR, relative permeability, and capillary pressure. This study noted that simulations without or with minimal levels of LGR showed injection well behavior inconsistent with those previously seen in field data for gas and water injection wells (by increasing injection rates through time rather than the expected decreasing injection rates through time) at a fixed BHIP (Xu and others, 2020; Finley and others, 2013). Different levels of areal cell size refinement were required within the LGR region before CO_2 injection well behavior was consistent with typical gas injection well behavior (depending on the relative permeability curves and injection conditions such as injection well BHIP). Expansion of the LGR beyond the parent cell containing the injection well was necessary in all conditions to accurately simulate the long-term CO_2 injectivity. Therefore, the main recommendations from this study regarding LGR are that CCS simulations should:

1) Include fit-for-purpose local grid refinement around injection wells to achieve expected early injection pressure and rate behavior.

2) Extend the LGR *region* beyond the parent grid cell containing the well until the average long-term injection rate is unchanged with further LGR region expansion.

3) Review the fit-for-purpose LGR after any changes to the simulation, including BHIP or injection rate constraints, to assure expected early injection well behavior is simulated.

These recommendations should be considered in the context of accurately representing the geologic system as well as any additional simulation parameters of interest, such as CO_2 dissolution. Proper fit-for-purpose LGR and LGR region sizing around all wells will result in simulations with accurate short- and long-term well injectivity for all injection conditions while minimizing the computational requirements for large-domain CCS simulations.

Additionally, capillary pressure should always be included in CCS simulations. This sensitivity study demonstrated that excluding capillary pressure in the simulations overpredicted the 12-year cumulative CO_2 injection by 10%–26% depending on simulated BHIPs. Greater overprediction occurred at lower BHIPs.

Finally, Bennion and Bachu's relative permeability curves, from the Basal Cambrian sandstone can be used as a substitute for site-specific data for other projects targeting the same Deadwood Formation or Basal Cambrian sandstone in the Williston Basin with a high degree of accuracy if site-specific relative permeability data are unavailable (Bennion and Bachu, 2005, 2007). Simulations showed very little difference in both low- and high-BHIP 12-year injectivity

predictions using Bennion and Bachu and site-specific relative permeability curves (Bennion and Bachu, 2005, 2007). This can aid in the acceleration of initial reservoir simulation and CCS site injection capacity estimates while waiting for site-specific relative permeability data to be acquired.

ACKNOWLEDGMENTS

This work was performed in support of the U.S. Department of Energy's SMART Initiative – Phase 1 through Leidos Inc.; IDIQ/Cost Reimbursable Term University (Federal) Subcontract Agreement; Subcontract No. P010227025; which supports Leidos' work under Prime Contract No. 89243318CFE000003; that has been issued by Department of Energy National Energy Technology Laboratory. This material is also based upon work supported by DOE Cooperative Agreement No. DE-FE0031838; "PCOR Initiative to Accelerate CCUS Deployment" and the North Dakota Industrial Commission (NDIC) under Contract Nos. FY20-XCI-226 and G-050-96. The authors also acknowledge the license of products from Computer Modelling Group, Calgary, Alberta, Canada.

DISCLAIMERS

(A) Makes any warranty or representation, express or implied, with respect to the accuracy, completeness, or usefulness of the information contained in this report, or that the use of any information, apparatus, method, or process disclosed in this report may not infringe privately-owned rights; or
(B) Assumes any liabilities with respect to the use of, or the use of, or for damages resulting from the use of, any information, apparatus, method, or process disclosed in this report.

Reference herein to any specific commercial product, process, or service by trade name, trademark, manufacturer, or otherwise, does not necessarily constitute or imply its endorsement, recommendation, or favoring by the Industrial Commission of North Dakota. The views and opinions of authors expressed herein do not necessarily state or reflect those of the Industrial Commission of North Dakota.

REFERENCES

Bennion, B., and Bachu, S., 2007, Permeability and relative permeability measurements at reservoir conditions for CO_2–water systems in ultralow-permeability confining caprocks: Paper presented at the EUROPEC/EAGE Annual Conference and Exhibition, London, United Kingdom.

Bennion, B., and Bachu, S., 2005, Relative permeability characteristics for supercritical CO_2 displacing water in a variety of potential sequestration zones: Paper presented at the SPE Annual Technical Conference and Exhibition, Dallas, Texas.

Bosshart N.W., Azzolina, N.A., Ayash, S.C., Peck, W.D., Gorecki, C.D., Ge, J., Jiang, T., and Dotzenrod, N.W., 2018, Quantifying the effects of depositional environment on deep saline formation CO_2 storage efficiency and rate: International Journal of Greenhouse Gas Control, v. 69.

Bosshart, N., Pekot, L., Wildgust, N., Gorecki, C., Torres, J., Jin, L., Ge, J., Jiang, T., Heebink, L., Kurz, M., Dalkhaa, C., Peck, W., and Burnison, S., 2018, Plains CO_2 Reduction (PCOR) Partnership—best practices for modeling and simulation of CO_2 storage: Grand Forks, North Dakota, University of North Dakota Energy & Environmental Research Center.

Cavanagh, A., 2013, Benchmark calibration and prediction of the Sleipner CO_2 plume from 2006 to 2012: Energy Procedia, v. 37, p. 3529–3545.

Ding, E., Harrison, P., Dozzo, J., and Lin, C., 2009, Prudhoe Bay—rebuilding a giant oil and gas full field model: Paper presented at the SPE Western Regional Meeting, San Jose, California.

Dogru A., Fung, L., Al-Shaalan, T., Middya, U., and Pita, J., 2008, From mega-cell to giga-cell reservoir simulation: Society of Petroleum Engineers. p. 1–19.

Dogru A., Fung, l., Middya, U., Al-Shaalan, T., Byer, T., Hoy, H., Hahn, W., Al-Zamel, N., Pita, J., Hemantkumar, K., Mezghani, M., Al-Mana, A., Tan, J., Dreiman, W., Fugl, A., and Al-Baiz, A., 2011, New Frontiers in Large Scale Reservoir Simulation: Society of Petroleum Engineers. p. 1–12.

617 Earlougher, R., 1977, Advances in well test analysis, Dallas: American Institute of Mining,
618 Metallurgical, and Petroleum Engineers, 264 p.

619 Finley, R., Frailey, S., Leetaru, H., Senel, O., Coueslan, M., and Marsteller, S., 2013, Early
620 operational experience at a one-million tonne CCS demonstration project, Decatur, Illinois:
621 Energy Procedia, v. 37, p. 6149–6155.

622 Gorecki C.D., Liu, G., Braunberger, J., Klenner, R., Ayash, S., Dotzenrod, N., Steadman, E.A.,
623 and Harju, J.A., 2014, Subtask 2.17 – CO_2 storage efficiency in deep saline formations:
624 Grand Forks, North Dakota, Energy & Environmental Research Center.

625 Internal Revenue Service, 2020, Credit for carbon oxide sequestration TD 9944:
626 www.irs.gov/pub/irs-drop/td-9944.pdf (accessed October 2021).

627 LeFever, R., Thompson, S., and Anderson, D., 1987, Earliest paleozoic history of the Williston
628 Basin in North Dakota: 5th International Williston Basin Symposium, p. 22–36.

629 Lim, M., Pope, G., and Sepehmoori, K., 1997, Grid refinement study of a hydrocarbon miscible
630 gas injection reservoir: Paper presented at the SPE Asia Pacific Oil and Gas Conference,
631 Kuala Lumpur, Malaysia.

632 Nilsen, H., Herrera, P., Ashraf, M., Ligaarden, I., Iding, M., Hermanrud, C., Lie, K.-T.,
633 Nordbotten, J., Dahle, H., and Keilegavlen, E., 2011, Field-case simulation of CO_2-plume
634 migration using vertical equilibrium models: Energy Procedia, v. 4, p. 3801–3808.

635 Pruess, K., and Nordbotten, J., 2011, Numerical simulation studies of the long-term evolution of
636 a CO_2 plume in a saline aquifer with a sloping caprock: Transport in Porous Media, v. 90,
637 p. 135–151.

638 Qi, R., LaForce, T., and Blunt, M., 2009, Design of carbon dioxide storage in aquifers:
639 International Journal of Greenhouse Gas Control, v. 3, p. 195–205.

640 Rego, F., Botechia, V., Correia, M., and Schiozer, D., 2016, Quantification of simulation model
641 grid size impact on polymer flooding application in heavy oil heterogeneous reservoir: Paper
642 presented at the SPE Trinidad and Tobago Section Energy Resources Conference, Port of
643 Spain, Trinidad and Tobago.

644 Rohmer, J., Issautier, B., Chiaberge, C., and Audigane, P., 2013, Large-scale impact of CO_2
645 storage operations—dealing with computationally intensive simulations for global
646 sensitivity analysis: Energy Procedia, v. 37, p. 3883–3890.

647 Samantray, A., Dashti, Q., Ma, E., and Kumar, P., 2003, Upscaling and 3D streamline screening
648 of several multimillion-cell earth models for flow simulation: SPE Reservoir Evaluation and
649 Engineering, v. 9, no. 1, p. 15–23.

650 Senel, O., and Chugunov, N., 2013, CO_2 injection in a saline formation—pre-injection reservoir
651 modeling and uncertainty analysis for Illinois Basin – Dacatur project: Energy Procedia,
652 v. 37, p. 4598–4611.

Stork, A., Nixon, C., Hawkes, C., Birnie, C., White, D., Schmitt, D., and Roberts, B., 2018, Is CO_2 injection at Aquistore aseismic? a combined seismological and geomechanical study of early injection operations: International Journal of Greenhouse Gas Control, v. 75, p. 107–124.

U.S. Environmental Protection Agency, 2018, Underground Injection Control (UIC) Program Class VI implementation manual for UIC program directors, January 2018–2020: www.epa.gov/sites/default/files/2018-01/documents/implementation_manual_508_010318.pdf (accessed July 2022).

Wildgust, N., Nakles, D., Bosshart, N., Heebink, L., Klenner, R., and Battle, E., 2018, Plains CO_2 Reduction (PCOR) Partnership—best practices for the technical assessment of geologic CO_2 storage: University of North Dakota: Grand Forks, North Dakota, Energy & Environmental Research Center.

Xu X., BinAmro, A., and Mabrook, M., 2020, Miscible gas injection EOR, carbonate reservoirs well injectivity field cases: Paper presented at the Abu Dhabi International Petroleum Exhibition & Conference, Abu Dhabi, United Arab Emirates.